Seismic detection of euroquakes originating from Europa's silicate interior

A.G. Marusiak[1], M.P. Panning[1], S.D. Vance[1], C. Nunn [1], S. C. Stähler[2], S. Tharimena[3]

[1]Jet Propulsion Laboratory, California Institute of Technology 4800 Oak Grove Drive, Pasadena CA, USA 91109
[2]Institute of Geophysics, ETH Zürich; Zürich, Switzerland
[3]Faculty of Earth Sciences, Geography and Astronomy, University of Vienna, Austria

Key Points:

- Seismic events from Europa's silicate interior could reveal interior composition and structure
- The subsurface ocean will likely dampen events and filter out shear waves
- A euroquake will likely need to be over a M_w 5.0 to be detectable by current seismic instrumentation

Corresponding author: Angela G Marusiak, marusiak@jpl.nasa.gov, angela.marusiak@gmail.com

Abstract

Detecting a seismic event from Europa's silicate interior would provide information about the geologic and tectonic setting of the moon's rocky interior. Reflections off a metallic core would indicate the presence, size, and state of the hypothesized core. However, the subsurface ocean will attenuate the signal, possibly preventing the waveforms from being detected by a surface seismometer. Here, we investigate the minimum magnitude of a detectable event originating from Europa's silicate interior. We analyze likely signal-to-noise ratios and compare the predicted signal strengths to current instrument sensitivities. We show that a magnitude $M_w \geq 3.5$ would be sufficient to overcome the predicted background noise. However, a minimum magnitude of $M_w \geq 5.5$ would be required for current instrumentation to be able detect the event. A thinner ice shell transmits greater ground acceleration amplitudes than a thicker ice shell, which might allow for $M_w \geq 4.5$ to be detectable.

1 Plain Language Summary

Europa, one of Jupiter's moons, has an icy surface overlying a subsurface ocean and rocky interior. Europa's surface is likely geologically active and its rocky interior may also produce seismic events. Here, we investigate if a data from a seismometer could detect and record signals originating from the rocky interior, thus allowing a science team to accurately determine if the interior is also geologically active. We model the potential signal strengths of an event from the deep interior, and compare the signal amplitude to predicted background noise and instrument capabilities. We find that an event with a magnitude of at least a 3.5 would overcome background noise. However, current instrumentation would require an event of at least a magnitude 5.5 to be detectable from anywhere on Europa's surface. If such an event were to occur, a seismometer on Europa's surface may be able to use the recorded signal to constrain the near-surface and deep interior structure, and also to study the geologic setting and activity of the rocky interior.

2 Introduction

Jupiter's moon Europa is of high scientific interest for several reasons. Europa has a surface ice layer overlying a potentially habitable subsurface ocean (Reynolds et al., 1983). Europa's surface is covered in fractures and faults, with few craters (Schenk & Mckinnon, 1989; Hoppa et al., 1999; McEwen, 1986) suggesting an active and geologically young surface (Bierhaus et al., 2009; Zahnle et al., 2003). Many of Europa's surface features are likely caused by tidal forces between Jupiter, Europa, and other Galilean moons, Io and Ganymede, which share a resonance with Europa (Greenberg et al., 1998, 2003; Hurford & Greenberg, 2005; Lee et al., 2005). Due to the great interest in the search for life in icy ocean worlds, there are planned missions such as ESA's JUpiter ICy moons Explorer (JUICE)(Grasset et al., 2013) and NASA's Europa Clipper (Phillips & Pappalardo, 2014) as well as conceptual missions including the Europa lander (Hand et al., 2017). These missions would explore Europa's ice shell and subsurface ocean through several geophysical investigations. A seismometer on a lander could record seismic events originating from Europa's interior and surface (Pappalardo et al., 2013; Lee et al., 2003). The primary science goals of a seismic investigation are to constrain interior structure—mainly the thickness of the ice shell and depth of the ocean—and to determine the level of Europa's seismicity.

Published estimates place Europa's ice shell between 5-50 km thick overlying an ocean roughly 125 km deep (Green et al., 2021; Quick & Marsh, 2015; Vilella et al., 2020; Billings & Kattenhorn, 2005; Howell, 2020). These studies mostly rely on thermodynamic and geophysical modeling, and observations of geologic surface features. The thickness of the ice shell depends on the temperature of the ice-ocean interface and the compo-

sition of the ocean and ice. The temperature profile will affect the seismic velocity profile of Europa as well as the waveform characteristics. On icy ocean worlds, seismic velocities through ice are expected to have a negative gradient such that velocities decrease with depth (Vance, Panning, et al., 2018). Surface waves will be influenced by this gradient, and Rayleigh and Crary waves have characteristic frequencies which depend on the ice shell thickness. Thicker ice shells ($\geq$20 km) are predicted to allow convection to occur within the ice shell. Convection alters the thermal profile the ice shell by increasing the thermal gradient in the near-surface, and maintaining a higher temperature in the convective regime. The changes in temperature reduce the seismic quality (increasing attenuation) (Cammarano et al., 2006). For these reasons, seismic waves traveling in a thinner ice shell will likely have stronger ground motion at lower frequencies compared to a thicker ice shell (Panning et al., 2018; Maguire et al., 2021).

Even a seismometer on a short-lived lander would likely record numerous seismic events. Previous studies have estimated that Europa could experience higher rates of seismicity than Earth (Panning et al., 2018; Hurford et al., 2020). Europa's seismicity is likely driven by diurnal tides, which would produce frequent but low magnitude events, and non-synchronous rotation, which produce less frequent but potentially higher magnitude events up to magnitude $\approx$ 5.3 (Nimmo & Schenk, 2006) or $\approx$ 6.0 (Panning et al., 2006), depending on the shear modulus of the ice shell. In addition to events in the surface ice shell, seismic events may occur in Europa's silicate interior. Here, we refer to seismic events as euroquakes (short for Europa-quake) to include events that occur both in the ice shell, normally referred to as icequakes, and in Europa's silicate interior.

However, understanding the detection limits of deep seismic events is paramount for understanding Europa's thermal history and its habitability. Detected seismic information from Europa's silicate interior would help reveal the current state of geologic activity of the silicate interior. Clusters of euroquakes could point to magmatic activity near the rock-ocean boundary, or to tidal dissipation near the boundary with the core (if it exists). These euroquakes could hint at the required heat flux and rheology of the interior, which in turn could be used to infer elemental inventory and mineralogy. Confirming the presence of hydrothermal or magmatic euroquakes would also have implications for the habitability of Europa's ocean, as such activity could supply thermal energy and key elements for life to exist (Vance et al., 2016; Barge & White, 2017). A recent study by Běhounková et al. (2021) suggests that tidal forces might create large magmatic pulses analogous to Large Igneous Provinces (LIPS). On Earth, LIPs are large intraplate volcanic events which may be tied to magma plumes and were responsible for widespread extinction events (Ernst, 2014). Lindström et al. (2015) suggests that strong seismic events likely occurred when magma moved within the near surface and erupted. Magmatic pulses or hydrothermal activity on Europa (Lowell & DuBose, 2005), as have also been hypothesized to occur in Enceladus (Choblet et al., 2017; Waite et al., 2017), would produce seismic activity. On Earth, volcanic seismicity (McNutt & Roman, 2015; McNutt, 1996) and seismic events from hydrothermal activity (Tolstoy et al., 2008) are well documented.

In addition to magma-driven seismic events, Europa may also experience deep euroquakes analogous to the deep tidally-driven moonquakes recorded by Apollo seismometers (Goulty, 1979; Bulow et al., 2007). Deep moonquakes (700-1000 km), the most commonly occurring seismic event on the Moon, tend to be located in clusters deep in the lunar mantle. These deep moonquakes have only been observed on the near-side, possibly due to a detection bias resulting from stations being deployed only on the near-side (Nunn et al., 2020), or due to heterogeneity within the Moon's deep interior (Nakamura, 2005).

Here, we model seismic events originating in Europa's silicate interior with ice shells ranging from 5 to 50 km. Our goals are to 1) compare the waveforms of deep euroquakes (depth = 155 km) to shallow euroquakes in the ice shell (depth = 3 km) to investigate

any reduction in ground motion amplitudes, 2) use realistic noise models (Panning et al., 2018) to determine the magnitude of a deep euroquakes needed to provide a sufficient signal-to-noise ratio (SNR), 3) compare the signal strength of deep euroquakes to current instrument capabilities, and 4) investigate if ice thickness plays a role in detection limits. These goals will determine the minimum magnitude of a euroquake that could be detected by a future lander mission.

3 Methods

3.1 Interior Models

In order to generate models of seismic waveforms from Europa's interior, we create basic interior structure model with a range of possible ice shell thicknesses. We generate the interior models using *PlanetProfile* (Vance, Panning, et al., 2018)(Figure 1), an open-source code that creates geophysically and thermodynamically consistent radial models based on available constraints from spacecraft data. We assume the ice shell is composed of pure, solid, water and the ocean composition is standard reference seawater (Millero et al., 2008). We set the silicate interior to a chondritic composition with a bulk composition (in weight percent) of 45.93% SiO_2, 28.52% MgO, 19.66% FeO, 2.18%. CaO, 2.55% Al_2O_3, and 1.17% Na_2O. The solid metallic core is mostly iron, with 1% sulfur. The models vary only in ice shell thickness and temperature profile of the ice shell and ocean: from a minimum ice shell thickness of 5 km up to a maximum of 50 km and corresponding ice-ocean interface temperatures ranging from 266 K (50 km ice shell) to 271 K (5 km ice shell). The radius of the silicate interior is roughly consistent, such that a thinner ice shell has a thicker ocean and vice versa. Seismic velocities in the ice layers are calculated using the SeaFreeze library (Journaux et al., 2019), assuming a pure water ice composition and no porosity. In the ocean compressional sound speeds are computed using the Gibbs Seawater toolbox in TEOS-10 (McDougall & Barker, 2011). Attenuation in the ice shell is calculated using the approach of Cammarano et al. (2006). Seismic velocities in the silicate interior and core are calculated using the Perple_X library (Connolly, 2009, 2005).

3.2 Synthetic Waveforms

Once we generate the interior structure models with PlanetProfile, we use the seismic velocity models as inputs for AxiSEM (Nissen-Meyer et al., 2014) and Instaseis (van Driel et al., 2015) (Figure 2). We set the dominant period to 1 second and create waveforms 3600 seconds long. This time and period allow us to best characterize multiple reflections off the ice-ocean interfaces, as well as seismic phases passing through and reflecting off the silicate interior and core. We are also able to capture most of the major and minor arcs of surface waves. We space receivers every 1 degree over 180 degrees to fully encompass distance ranges. For each model, we set event depths at 3 km and 155 km, representing euroquakes originating in the icy shell and in the silicate interior near the ocean-rock boundary.

3.3 Background Noise

After we create the seismograms, background noise is added. We create time series waveforms using the preferred seismicity, catalog 0 model from Panning et al. (2018). It is worth noting that Panning et al. (2018) shows the expected background noise of Europa is significantly lower than Earth's New Low Noise Model (Peterson, 1993). This Europa noise model consists of single cracks following a Gutenberg-Richter distribution in size and random geographic locations in Europa's ice shell. The resulting time series of noise contains a larger euroquake with a maximum displacement amplitude of $\approx \pm 400$ nm and then time between euroquakes with amplitudes below $\approx \pm 0.1$ nm. To arrive at a

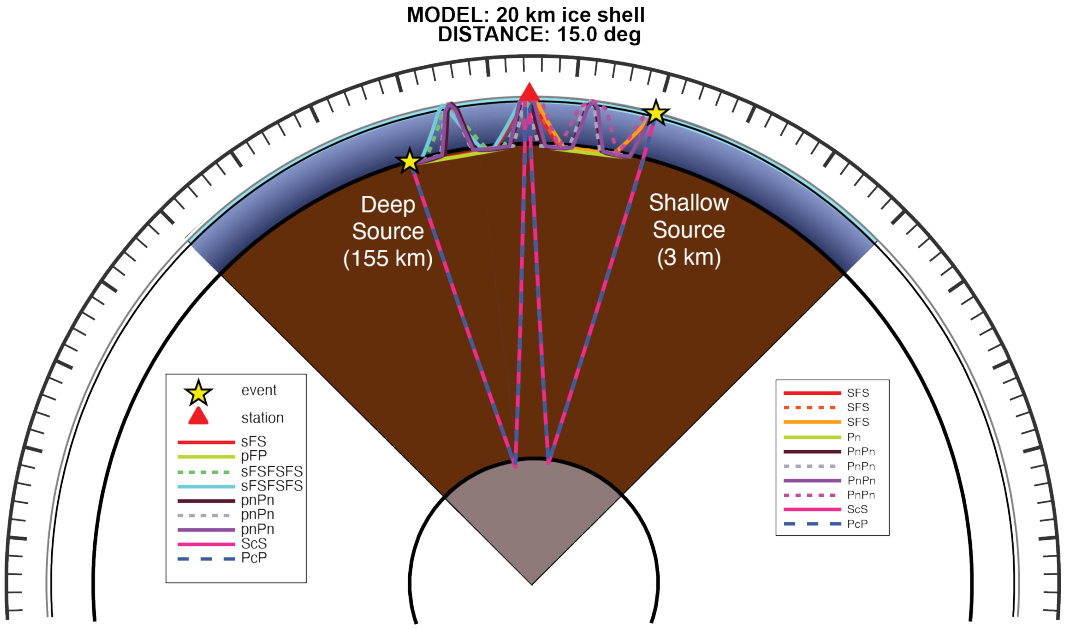

Figure 1. Example of seismic phases passing through the interior of Europa. On the left the euroquake (yellow star) occurs at a depth of 155 km and a distance of 15 degrees from the station (red triangle). On the right is a shallow euroquake at a depth of 3 km and a distance of 15 degrees. The ice shell (light blue) is 20 km thick, overlying an ocean (dark blue), silicate interior (brown, radius 1411 km), and metallic core (gray, radius 390 km). We generate the ray paths using a modified version of TauP (Crotwell et al., 1999). The seismic phases are labeled according to the nomenclature presented in Stähler et al. (2017) such that c refers to a core reflected phase, F are P waves in fluids. Note that different phases and triplications are seen for the deep versus shallow event.

temporally more homogeneous time series that still retains the spectral character, we perturb it as follows: We calculate the Fourier-transform and power spectral density of the original time series to determine the mean value across a broad frequency band (0.002 - 3 Hz). We then perform an inverse fast Fourier-transform to convert the mean power back into a time series. This new time series represents an average value for background noise with a maximum value of $\approx \pm 0.5$ nm, rather than the large variability of the original time series. The final time series of noise is added to each of the euroquake waveforms to create a realistic seismic signal that a seismometer might record on Europa's surface. Once we add the noise, we assess whether the signal strength is greater than the background, assigning an SNR according to Equation 1. We use the absolute value of the ground acceleration amplitude to account for any negative values in amplitude. The root mean square (rms) provides an average value for the background noise level.

$$SNR = \frac{|RecordSignal|}{rms(BackgroundNoise)} \tag{1}$$

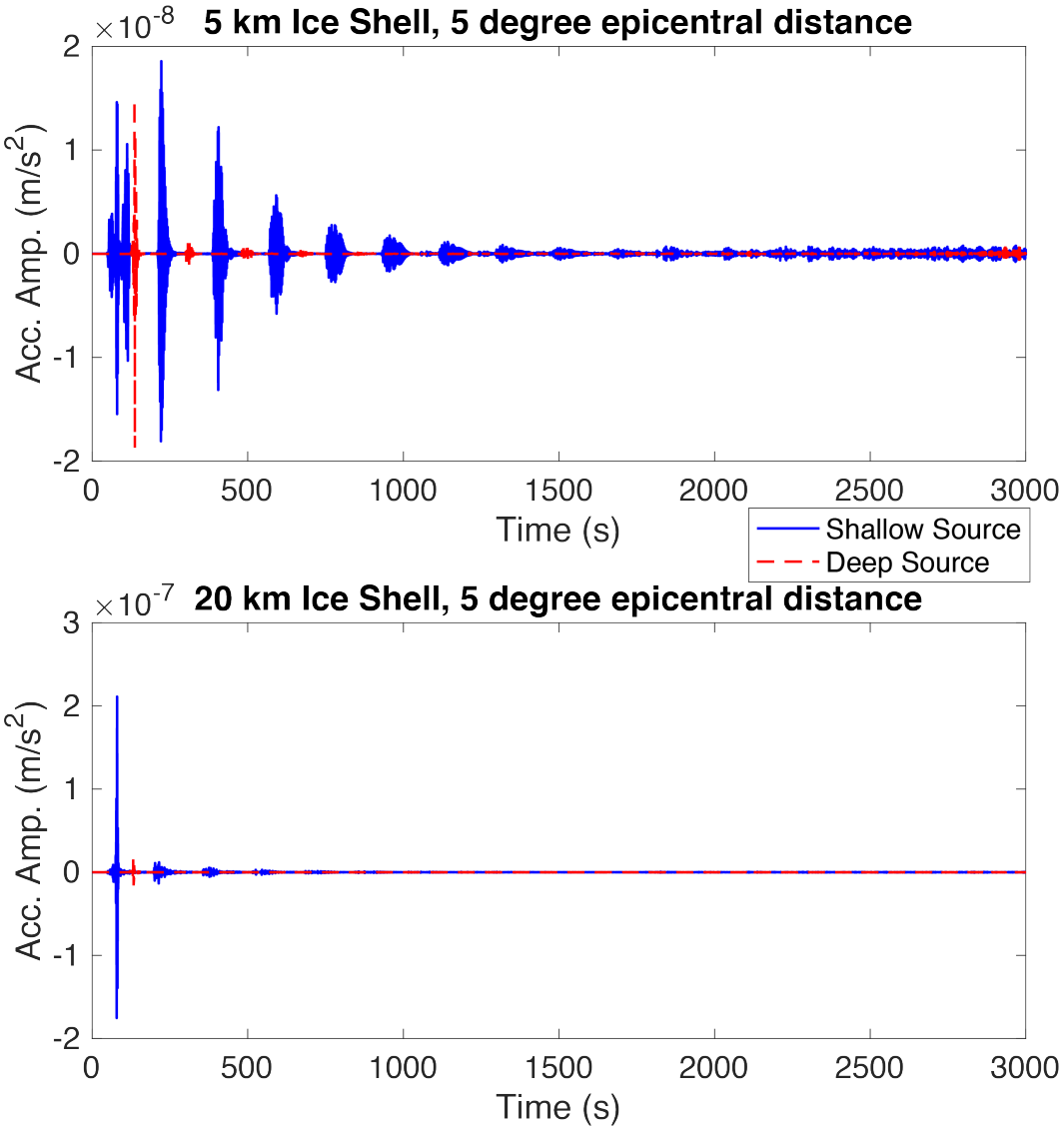

Figure 2. Comparison of raw waveforms from models with different ice shell thicknesses and event depths. Note the difference in y-axis scale. A deeper euroquake (red) has smaller arrivals compared to a more shallow event (blue).

4 Results

4.1 Surface vs Deep comparison

We first compare waveforms without added noise (Figure 3). The acceleration amplitudes are smaller by a factor of 2.5-10 for a thinner ice shell, but a thicker shell has even greater reductions of 12-140x for a deep versus shallow euroquake. The vertical component tends to have slightly lower reductions in amplitude compared to the radial component. We choose not to show to show the transverse component since shear waves do not travel through the ocean. The resulting waveform is mostly numerical noise and would be difficult to interpret correctly. A seismometer placed on Europa's surface would be able to measure the transverse component due to scattering effects in Europa's ice shell.

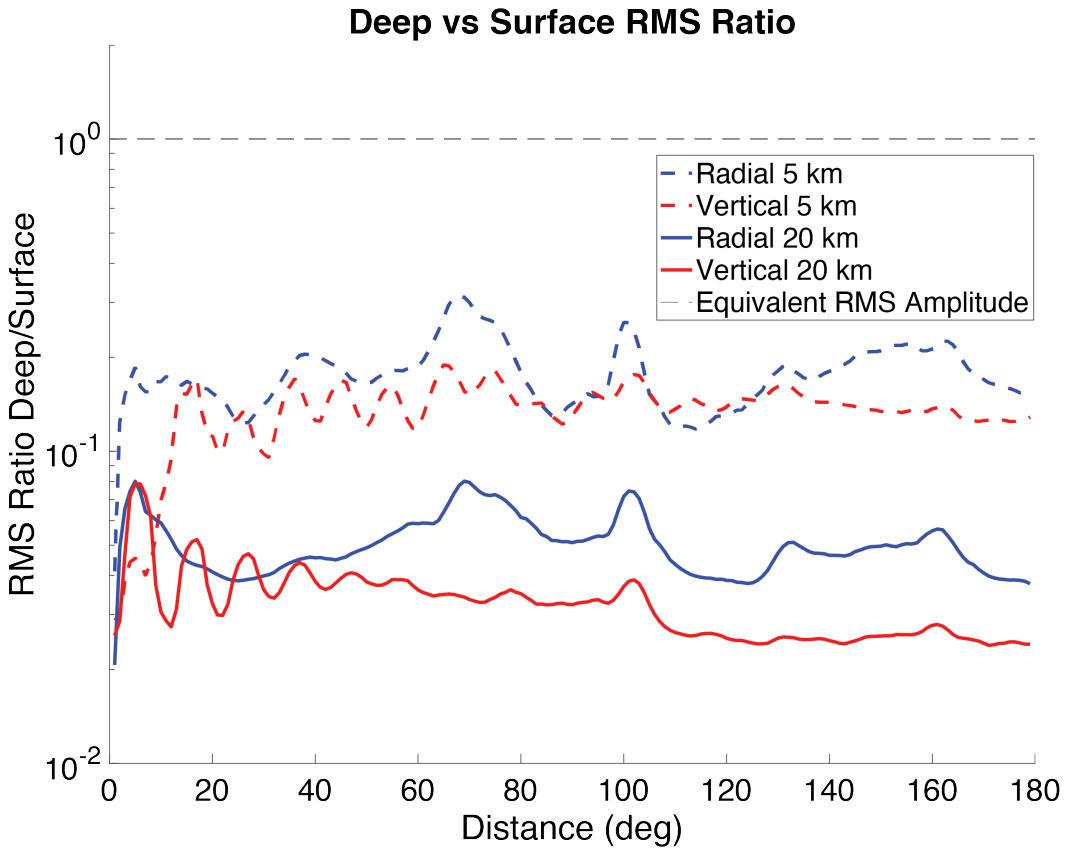

Figure 3. Ratio of the acceleration amplitudes between shallow (3 km) and deep (155 km) euroquakes. Both radial (blue) and vertical (red) components are shown for a 20 km (solid) and a 5 km (dashed) ice shell. For each distance, the ratio of the root mean square (RMS) for the deep event to the RMS of the shallow event is displayed. We smooth the values over 5 degrees to reduce the effects of constructive/deconstructive interference when seismic phases overlap. The 5 km shell shows deep euroquakes have amplitudes about one tenth of shallow euroquakes amplitudes, while the 20 km ice shell shows an even greater reduction in amplitudes.

However, our modeling does not include the effects of scattering, as it would be too computationally expensive for the global scale of our investigation.

4.2 Realistic Noise estimation

We use the preferred seismicity model and catalog 0 from Panning et al. (2018), along with the AxiSem generated databases we generated for each ice shell thickness, to determine if a signal from a deep euroquake could be resolved over a background signal. For both shallow and deep euroquakes we test several magnitude euroquakes with the same background signal to determine which euroquakes have visible signals. At a distance of 10 degrees, a M_w 3.0 euroquake, cannot easily been seen in the raw seismograms, and would require additional filtering and signal processing. At the same distance, high ground acceleration amplitude phases from a deep euroquake can be seen on both the radial and vertical for a M_w 3.5 (Figure 4a,i, but many phases aren't readily visible until $M_w \geq 4.0$ (Figure 4b,f).

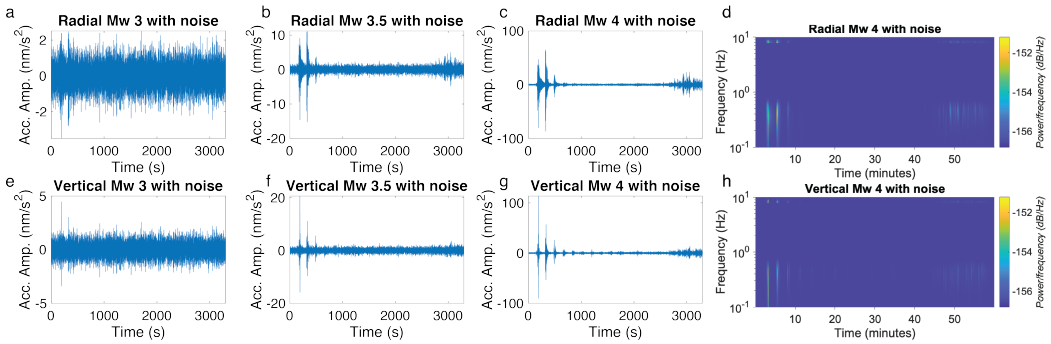

Figure 4. All euroquakes are for a 10 km ice shell with a 155 km source depth. Different magnitude deep euroquakes (columns) with the same background noise are plotted for both the radial (top row) and vertical components (bottom row). Plots *d* and *h* show spectrograms for the time series in *c* and *g*, respectively.

In addition to viewing the time series data to identify an event, a common approach is to use periodograms or spectrograms to view the signals in the frequency domain. This approach is being used by the InSight mission to identify marsquakes (Giardini et al., 2020). Background noise tends to dominant at high frequencies, while euroquakes tend to dominant at longer periods and lower frequencies. When spectra indicate high power at low frequencies, this can indicate there is a seismic event. We apply this approach to determine if small magnitude euroquakes could be more identifiable in the frequency domain than in the time domain. We use a frequency range of 0.7-2 Hz. Here we show how a M_w 4.0 euroquake can be seen easily on the spectrogram with signal strengths several decibels over background noise. A signal that is difficult to see in the time series is not necessarily easier to see in the spectral domain. A M_w 3.5 deep euroquake with a 10 km ice shell has phases that are only about a decibel or two above the background noise.

Overall, the SNR depends both on the magnitude of the euroquake and the thickness of the ice shell. Although a M_w 3.5 euroquake has high SNRs when the ice shell is 5 km thick (Fig. 5 a), the SNRs are much lower when the ice shell thickness increases to 35 km (Fig. 5 b). For thicker ice shells, a $M_w \geq 4.0$ may be required in order to identify key body wave phases from any distance.

4.3 Comparison to Instrument Capabilities

Although a deep euroquake may have a sufficient SNR relative to ambient seismic noise, that does not guarantee a seismometer would be able to record its signal. Panning et al. (2018) show that several candidate instruments are unlikely to record Europa's background noise due to the low ground acceleration amplitudes of the signals (predominately $M_w \leq 2.5$) compared to instrument self-noise. We test different magnitudes to determine the required signal strength to be detected by several seismic instruments (Figure 7) and investigate whether the ice shell thickness affects the detectability. For simplicity we use the noise floor of a Trillium Compact (TC), a broadband STS2 seismometer, the Silicon Seismic Package (SSP) (a lunar microseismometer currently being developed (Nunn et al., 2021)) and InSight's SEIS Short Period sensor (SP) (Mimoun et al., 2017) recorded noise levels during its flight to Mars. We assume the seismometer would only record the signal plus the added background noise; we do not add in lander noise or noise from other instrumentation.

Although a M_w 3.5 euroquake is sufficient to rise above the background noise (at least for thinner ice shells (< 20 km)), a euroquake of that size is unlikely to be recorded

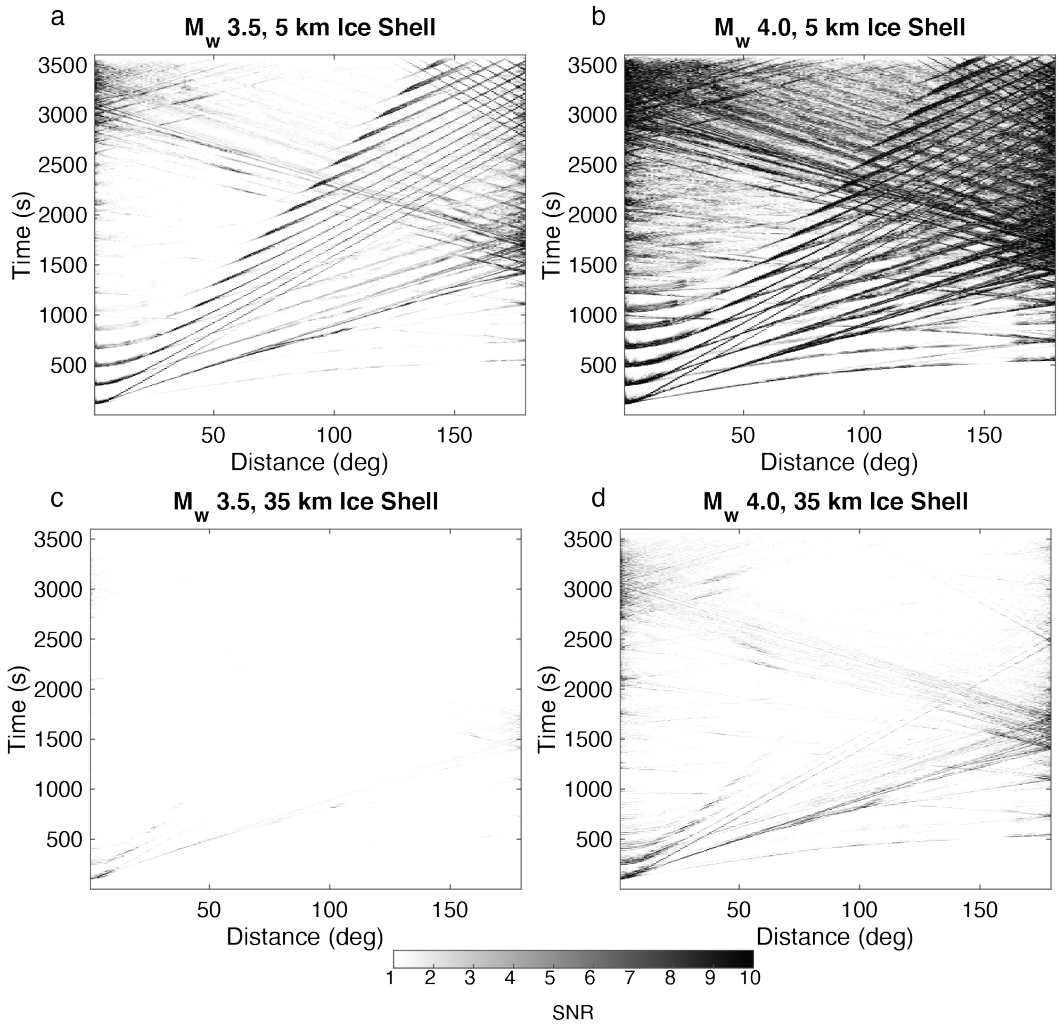

Figure 5. SNRs against ambient noise for deep source euroquake M_w 3.5 (a,c) and M_w 4.0 (b,d) for a 5 km (a,b) and 35 km (c,d) thick ice shell. The vertical components can easily be seen at most distances with a M_w 3.5 with a thinner ice shell, but are not easily visible until a M_w 4.0 with a thicker ice shell. Gray scale bar is set so an SNR of 0 (meaning signal equals noise) is white and the scale saturates at SNR of 10.

by even an STS2 seismometer, one of the more sensitive instruments used in terrestrial deployments. As seen in Figure 7, at a distance of 10 degrees, a M_w 4.5 euroquake propagating through a 20 km ice shell, can be detected by sensitive instruments but not the TC or SP instruments. A M_w 5.0 euroquake would be required to be detectable over a wide range of distances by the less sensitive instruments. It is plausible a M_w 4.5 euroquake might be detectable by more sensitive equipment if it happens to occur within a short epicentral distance and the ice shell is thinner than 35 km. A M_w 5.0 euroquake could be recorded by an STS2 or SSP, regardless of ice shell thickness.

The detection of a deep euroquake will be highly dependent on ice shell thickness. Thinner ice shells maintain higher amplitude seismic waves compared to thicker ice shells over a range of distances. In Figure 3 we show a deep source, M_w 5.0 euroquake is globally detectable if the ice shell is $\leq$ 20 km. For the 5 km and 10 km ice shell models, the euroquake produces signals that are over 10 dB above the detection threshold for the TC.

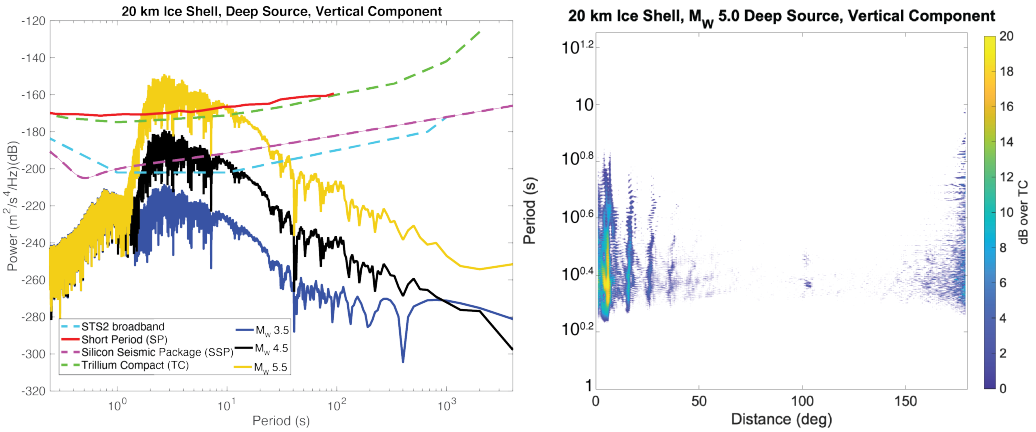

Figure 6. left) Comparison of vertical component acceleration amplitudes using the 20 km ice shell model for M_w 3.5 (blue), M_w 4.5 (black), and M_w 5.0 (yellow) euroquakes at an epicentral distance of 10 degrees. The short-period seismometer of the InSight mission (Lognonné et al., 2019) (red), Trillium Compact (TC) (dashed green) are the least sensitive instruments shown here. The STS2 (dashed cyan) and Silicon Seismic Package (SSP, dashed magenta) are more sensitive. The M_w 3.5 euroquake is not detectable, but the M_w 4.5 euroquake could be detected by STS2 and SSP. All instruments could detect the M_w 5.0 euroquake. Right) The strength of a M_w 5.0 signal in a 20 km ice shell compared to the TC instrument over all distances and periods between 1-15 seconds, the period range most likely to record a signal. While the M_w 5.0 euroquake can be seen at most distances, a thicker ice shell would require a $M_w \geq 5.5$ euroquake to be globally detected.

The same euroquake can be detected at most distances with a 35 km ice shell but only at distances $\leq$ 20 degrees or $\geq$ 170 degrees with a 50 km ice shell.

5 Discussion

Euroquakes originating from Europa's deeper interior will have reduced ground acceleration amplitudes compared to near-surface euroquakes, by a factor of 3-140 depending on the distance from the source and thickness of the ice shell. Deep euroquakes have surface waves that are more difficult to identify, as their amplitudes are severely dampened by the ocean and less energy is trapped within the ice shell. Thicker ice have a greater reduction in amplitude than thinner ice shells. The greater reduction in amplitudes is likely due to warm convecting ice which has greater attenuation than cold brittle ice found in thin ice shells.

5.1 Limitations of Models

To be globally detectable by flight-candidate seismometers, a euroquake with a deep source and ice shell thinner than 35 km needs to be at least a M_w 5.0. For this investigation, we compare euroquakes with deep source depths to euroquakes with shallow sources. Our main assumption is that the ice shell is laterally homogeneous and that there is no topography along any boundary. Although we assume Europa's ice shell is solid, pure water ice, the ice likely contains some impurities (Kargel et al., 2000), including the possibility of clathrate hydrates (Hand et al., 2006). Uneven distribution of impurities within Europa's ice shell should have only minor effects on seismic quality factors and

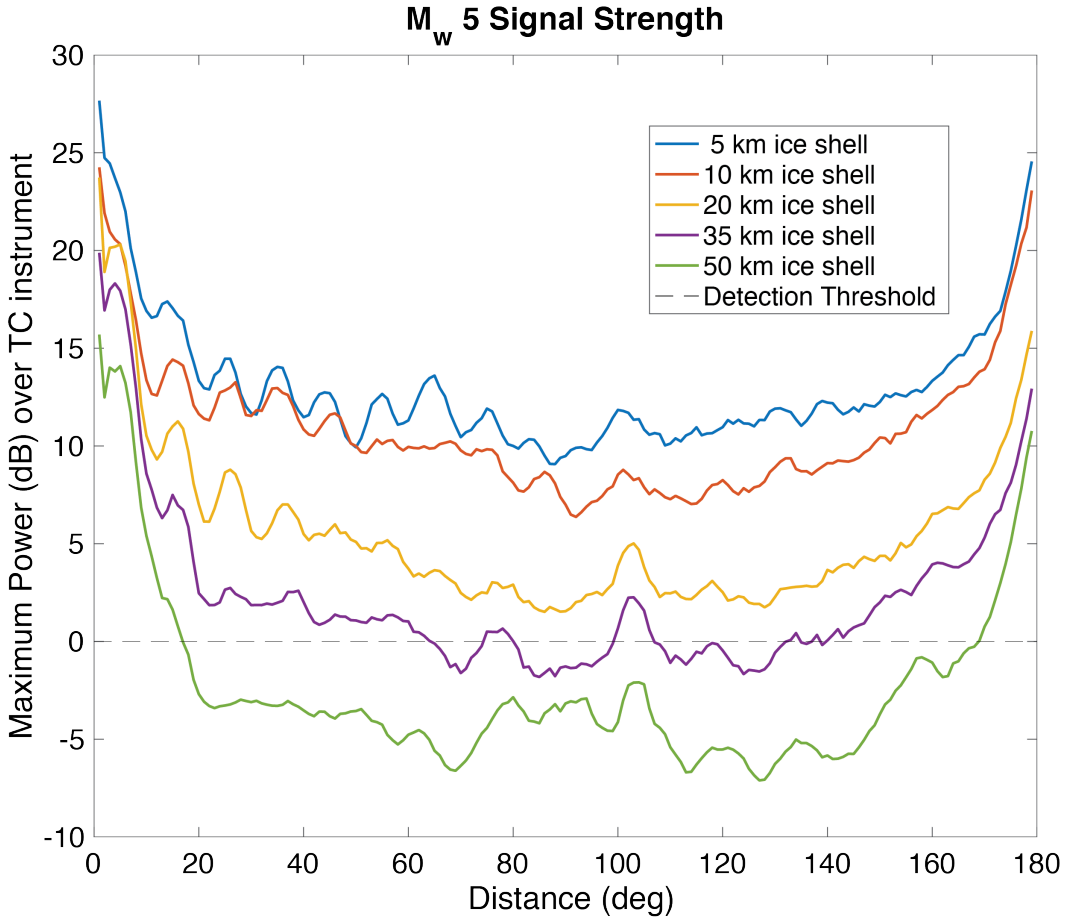

Figure 7. Signal strength of a M_w 5.0 euroquake based on ice shell thickness and distance. A value above 0.0 indicates the signal strength exceeds detection limits for a Trillium Compact (TC)-like instrument. A 5 km (blue), 10 km (red), and 20 km (yellow) ice shell are globally detectable. However, a 35 km ice shell would only allow a signal from a M_w 5.0, deep source euroquake, to be detectable at certain ranges. Likewise, a 50 km ice shell suppresses the euroquake's signal at distances greater than 20 degrees and less than 170 degrees.

scattering, and are unlikely to reduce waveforms' amplitudes at Europa's surface—our main criteria for detection.

We initially investigated the effects of porosity but our investigation revealed that the ground acceleration amplitudes of the euroquakes are not strongly reduced, but it is likely we have underestimated the effects. Porosity decreases seismic velocities and creates a scattering effect that can make it difficult to identify body waves. Lunar seismic investigations have been hampered by the strong scattering effects (Dainty et al., 1974; Nakamura, 1977). For this reason, we wanted to test if porosity would increase the minimum magnitude of a euroquake that could be detected. However, the investigation was limited in that we modeled changes in velocity and density but not scattering effects. We would need to use three-dimensional modeling or reduce the scale of our investigation to a local or regional scale to properly account for scattering effects that can reduce amplitudes further. Because of the limitations of our modeling, we do not show the results of the porosity investigations.

5.2 Instrumentation Capabilities

Several of the instruments, including the commercial Trillium Compact, are more sensitive at higher frequencies ($\geq$ 1 Hz), not pictured here. Our synthetic waveform modeling approaches are limited to lower frequencies. Higher frequencies are more computationally expensive, and thus we limit ourselves to a dominant period of 1 s (1 Hz). The less sensitive instruments might be able to detect smaller euroquakes than our study predicts, particularly if the euroquakes are located at short distances that lead to retaining more of the high frequency signal. More sensitive equipment might be able to detect a M_w 4.5 euroquake over a larger range of distances. Flight candidate seismometers under development, such as the Seismometer to Investigate Ice and Ocean Structure (Marusiak et al., 2020, 2021), the Europa Seismic Package (Kedar et al., 2020), and the SSP (Nunn et al., 2021) may improve the chances of detecting a deep euroquake.

The Europa lander mission concept (Hand et al., 2017) uses the detection limits of the Trillium Compact as a guide for the seismic instrument payload. On this basis, a magnitude M_w 4.5 euroquake might be detected if the euroquake has a small epicentral distance and the ice shell is relatively thin ($\leq$ 10 km). An additional difficulty arises from the lander concept design, which places the seismometer in the lander vault to protect from Europa's harsh surface radiation. Terrestrial analog studies in icy ocean world locations (Marusiak et al., 2021, 2020) and in martian settings (Panning et al., 2020) show that placing seismometers on lander decks can introduce coda and additional noise, although these effects are greatly reduced in the absence of wind. The additional noise from the lander resonant frequencies tends to occur at high frequencies ($\geq$ 50 Hz) and depends on specifics of the lander design and placement of the seismometer (Marusiak et al., 2021). Placing seismometers on lander decks can add $\approx$ 20 dB of noise at the lander's resonant frequencies, but otherwise lander-based instrumentation records signals within 5 dB of a surface coupled seismometer. For simplicity, we do not account for the added noise from on-deck placement.

Based on our results, a seismic euroquake with a deep source needs to be at least a M_w 5.0 to be globally detectable with a TC-like instrument for ice shells $<$ 35 km or at least a M_w 5.5 if the ice shell is $\geq$ 35 km. While such events are common on Earth, the two largest recorded moonquakes were a body wave magnitude 5.6 and 5.8 (Oberst, 1987), and they were shallow events. Although Europa is assumed to be more seismically active than the Moon (Vance, Kedar, et al., 2018), it is currently unknown whether the deep interior is capable of producing a euroquake large enough to be detected. Such an investigation is beyond the scope of this study. Additional analyses regarding the rheology, estimated tidal dissipation, and other physical parameters of the interior need to be studied in more detail to assess if the silicate interior could produce a sufficient event.

6 Summary and Conclusion

We test how euroquakes originating from Europa's silicate interior compare to euroquakes originating in Europa's icy shell. Compared to shallow euroquakes, deep euroquakes will have acceleration amplitudes 2-140x smaller. A euroquake from the interior could overcome background noise if the event's magnitude exceeds $M_w \geq 3.5$, but a $M_w \geq 4.0$ would allow for better identification of seismic waves regardless of ice shell thickness and epicentral distance between the source and seismometer. However, even sensitive seismic instrumentation would be unlikely to detect a euroquake with $M_w \leq$ 4.5, particularly if the ice shell is thick ($\geq$ 20 km). In order for a euroquake from Europa's silicate interior to be globally detected, regardless of ice shell thickness, it would likely need to be at least a M_w 5.5 to meet the capabilities of likely flight candidate seismometers. Further studies on the possible rheology and tidal dissipation within the rocky interior would help in determining if Europa's interior could produce an event with large

enough signals. Improvement in flight-candidate seismometers would also improve the chances of recording a euroquake from the interior.

Acknowledgments

A portion of this research was carried out at the Jet Propulsion Laboratory, California Institute of Technology, under a contract with the National Aeronautics and Space Administration (Habitable Worlds Grant: 16-HW16_2-0065) and JPL's Strategic Research and Technology Development program.

Files containing internal structures, SAC files, and code are available through : `https://github.com/agmarusiak/Europa_Deep_Events` DOI:10.5281/zenodo.5525009

References

Barge, L. M., & White, L. M. (2017, 9). Experimentally Testing Hydrothermal Vent Origin of Life on Enceladus and Other Icy/Ocean Worlds. *Astrobiology*, *17*(9), 820–833. Retrieved from `http://www.liebertpub.com/doi/10.1089/ast.2016.1633` doi: 10.1089/ast.2016.1633

Běhounková, M., Tobie, G., Choblet, G., Kervazo, M., Melwani Daswani, M., Dumoulin, C., & Vance, S. D. (2021, 2). Tidally Induced Magmatic Pulses on the Oceanic Floor of Jupiter's Moon Europa. *Geophysical Research Letters*, *48*(3), e2020GL090077. Retrieved from `https://doi.org/10.1029/2020GL090077` doi: 10.1029/2020GL090077

Bierhaus, E. B., Zahnle, K., Chapman, C. R., Pappalardo, R. T., McKinnon, W. R., & Khurana, K. K. (2009). Europa's crater distributions and surface ages. *Europa*, 161–180.

Billings, S. E., & Kattenhorn, S. A. (2005, 10). The great thickness debate: Ice shell thickness models for Europa and comparisons with estimates based on flexure at ridges. *Icarus*, *177*(2), 397–412. Retrieved from `https://linkinghub.elsevier.com/retrieve/pii/S0019103505001211` doi: 10.1016/j.icarus.2005.03.013

Bulow, R. C., Johnson, C. L., Bills, B. G., & Shearer, P. M. (2007). Temporal and spatial properties of some deep moonquake clusters. *Journal of Geophysical Research: Planets*, *112*(9), 1–12. doi: 10.1029/2006JE002847

Cammarano, F., Lekic, V., Manga, M., Panning, M. P., & Romanowicz, B. (2006). Long-period seismology on Europa: 1. Physically consistent interior models. *Journal of Geophysical Research-Planets*, *111*(E12). doi: ArtnE1200910.1029/2006je002710

Choblet, G., Tobie, G., Sotin, C., Běhounková, M., Čadek, O., Postberg, F., & Souček, O. (2017). Powering prolonged hydrothermal activity inside Enceladus. *Nature Astronomy*, *1*(12), 841–847. Retrieved from `https://doi.org/10.1038/s41550-017-0289-8` doi: 10.1038/s41550-017-0289-8

Connolly, J. A. D. (2005). Computation of phase equilibria by linear programming: A tool for geodynamic modeling and its application to subduction zone decarbonation. *Earth and Planetary Science Letters*, *236*(1), 524–541. Retrieved from `https://www.sciencedirect.com/science/article/pii/S0012821X05002839` doi: https://doi.org/10.1016/j.epsl.2005.04.033

Connolly, J. A. D. (2009). The geodynamic equation of state: what and how. *Geochemistry, Geophysics, Geosystems*, *10*(Q10014). doi: 10.1029/2009GC002540

Crotwell, H. P., Owens, T. J., & Ritsema, J. (1999, 3). The TauP Toolkit: Flexible Seismic Travel-time and Ray-path Utilities. *Seismological Research Letters*, *70*(2), 154–160. Retrieved from `https://pubs.geoscienceworld.org/srl/article/70/2/154-160/142385` doi: 10.1785/gssrl.70.2.154

Dainty, A. M., Toksoz, M. N., Anderson, K. R., Pines, P. J., Nakamura, Y., Latham,

G., ... Latham, G. (1974). Seismic scattering and shallow structure of the moon in oceanus procellarum. *The moon*, *9*(1), 11–29. Retrieved from https://doi.org/10.1007/BF00565388http://link.springer.com/10.1007/BF00565388 doi: 10.1007/BF00565388

Ernst, R. E. (2014). *Large igneous provinces*. Cambridge University Press.

Giardini, D., Lognonné, P., Banerdt, W. B., Pike, W. T., Christensen, U., Ceylan, S., ... Yana, C. (2020, 3). The seismicity of Mars. *Nature Geoscience*, *13*(3), 205–212. Retrieved from https://doi.org/10.1038/s41561-020-0539-8http://www.nature.com/articles/s41561-020-0539-8 doi: 10.1038/s41561-020-0539-8

Goulty, N. R. (1979). Tidal triggering of deep moonquakes. *Physics of the Earth and Planetary Interiors*, *19*(1), 52–58.

Grasset, O., Dougherty, M. K., Coustenis, A., Bunce, E. J., Erd, C., Titov, D., ... Van Hoolst, T. (2013). JUpiter ICy moons Explorer (JUICE): An ESA mission to orbit Ganymede and to characterise the Jupiter system. *Planetary and Space Science*, *78*, 1–21. Retrieved from https://www.sciencedirect.com/science/article/pii/S0032063312003777 doi: 10.1016/j.pss.2012.12.002

Green, A. P., Montesi, L. G., & Cooper, C. M. (2021). The Growth of Europa's Icy Shell: Convection and Crystallization. *Journal of Geophysical Research: Planets*, *126*(4), 1–22. doi: 10.1029/2020JE006677

Greenberg, R., Geissler, P., Hoppa, G. V., Tufts, B. R., Durda, D. D., Pappalardo, R. T., ... Carr, M. H. (1998). Tectonic Processes on Europa: Tidal Stresses, Mechanical Response, and Visible Features. *Icarus*, *135*, 64–78.

Greenberg, R., Hoppa, G. V., Bart, G., & Hurford, T. A. (2003). Tidal stress patterns on Europa's crust. *Celestial Mechanics & Dynamical Astronomy*, *87*(1-2), 171–188. doi: 10.1023/A:1026169424511

Hand, K. P., Chyba, C. F., Carlson, R. W., & Cooper, J. F. (2006, 6). Clathrate Hydrates of Oxidants in the Ice Shell of Europa. *Astrobiology*, *6*(3), 463–482. Retrieved from http://www.liebertpub.com/doi/10.1089/ast.2006.6.463 doi: 10.1089/ast.2006.6.463

Hand, K. P., Murray, A. E., Garvin, J. B., Brinckerhoff, W. B., Christner, B. C., Edgett, K. S., ... Team, P. E. (2017). *Report of the Europa Science Definition Team* (Tech. Rep.). Retrieved from https://europa.nasa.gov/resources/58/europa-lander-study-2016-report/

Hoppa, G. V., Tufts, B. R., Greenberg, R., & Geissler, P. (1999). Strike-slip faults on Europa: Global shear patterns driven by tidal stress. *Icarus*, *141*(2), 287–298. doi: 10.1006/icar.1999.6185

Howell, S. M. (2020, 8). The Likely Thickness of Europa's Icy Shell. In *European planetary science congress* (Vol. 2, pp. 2020–173). IOP Publishing. Retrieved from http://dx.doi.org/10.3847/PSJ/abfe10https://iopscience.iop.org/article/10.3847/PSJ/abfe10 doi: 10.3847/PSJ/abfe10

Hurford, T. A., & Greenberg, R. (2005). *Tides and Tidal Stress: Applications to Europa* (Unpublished doctoral dissertation).

Hurford, T. A., Henning, W., Maguire, R., Lekic, V., Schmerr, N. C., Panning, M. P., ... Rhoden, A. (2020, 3). Seismicity on tidally active solid-surface worlds. *Icarus*, *338*, 113466. Retrieved from http://www.sciencedirect.com/science/article/pii/S0019103518307243https://linkinghub.elsevier.com/retrieve/pii/S0019103518307243 doi: 10.1016/j.icarus.2019.113466

Journaux, B., Brown, J. M., Bollengier, O., Abramson, E., Tobie, G., & Vance, S. D. (2019). SeaFreeze : A modular thermodynamic framework for modeling all solar system planetary hydrospheres, including ice polymorphs and aqueous solutions at high-pressures. In *Epsc-dps.* Retrieved from https://meetingorganizer.copernicus.org/EPSC-DPS2019/EPSC-DPS2019-797-1.pdf

Kargel, J. S., Kaye, J. Z., Head, J. W. I. I. I., Marion, G. M., Sassen, R., Crowley, J. K., ... Hogenboom, D. L. (2000). Europa's Crust and Ocean: Origin, Composition, and the Prospects for Life. *Icarus*, *148*(1), 226–265. doi: 10.1006/icar.2000.6471

Kedar, S., Panning, M. P., Standley, I. M., Blaes, B. R., Walsh, W., Calcutt, S. B., ... Franklin, G. W. (2020, 12). The Europa Seismic Package. In *Agu fall meeting abstracts* (Vol. 2, pp. 044–0020). Retrieved from https://ui.adsabs.harvard.edu/abs/2020AGUFMP044.0020K/abstract

Lee, S., Pappalardo, R. T., & Makris, N. C. (2005). Mechanics of tidally driven fractures in Europa's ice shell. *Icarus*, *177*(2), 367–379.

Lee, S., Zanolin, M., Thode, A. M., Pappalardo, R. T., & Makris, N. C. (2003, 9). Probing Europa's interior with natural sound sources. *Icarus*, *165*(1), 144–167. Retrieved from https://linkinghub.elsevier.com/retrieve/pii/S0019103503001507 doi: 10.1016/S0019-1035(03)00150-7

Lindström, S., Pedersen, G. K., van de Schootbrugge, B., Hansen, K. H., Kuhlmann, N., Thein, J., ... Tegner, C. (2015, 5). Intense and widespread seismicity during the end-Triassic mass extinction due to emplacement of a large igneous province. *Geology*, *43*(5), 387–390. Retrieved from https://doi.org/10.1130/G36444.1 doi: 10.1130/G36444.1

Lognonné, P., Banerdt, W. B., Giardini, D., Pike, W. T., Christensen, U., Laudet, P., ... Wookey, J. (2019, 2). SEIS: Insight's Seismic Experiment for Internal Structure of Mars. *Space Science Reviews*, *215*(1), 12. Retrieved from http://link.springer.com/10.1007/s11214-018-0574-6 doi: 10.1007/s11214-018-0574-6

Lowell, R. P., & DuBose, M. (2005, 3). Hydrothermal systems on Europa. *Geophysical Research Letters*, *32*(5). Retrieved from https://doi.org/10.1029/2005GL022375 doi: 10.1029/2005GL022375

Maguire, R., Schmerr, N., Pettit, E., Riverman, K., Gardner, C., Della-Giustina, D., ... Bailey, H. (2021). Geophysical constraints on the properties of a subglacial lake in northwest Greenland. *The Cryosphere Discussions*, 1–19. doi: 10.5194/tc-2020-321

Marusiak, A. G., Schmerr, N. C., DellaGiustina, D. N., Avenson, B., Bailey, S. H., Bray, V. J., ... Weber, R. C. (2021, 3). The Deployment of the Seismometer to Investigate Ice and Ocean Structure (SIIOS) in Northwest Greenland: An Analog Experiment for Icy Ocean World Seismic Deployments. *Seismological Research Letters*. Retrieved from https://pubs.geoscienceworld.org/ssa/srl/article/595406/The-Deployment-of-the-Seismometer-to-Investigate doi: 10.1785/0220200291

Marusiak, A. G., Schmerr, N. C., DellaGiustina, D. N., Pettit, E. C., Dahl, P. H., Avenson, B., ... Weber, R. C. (2020, 5). The Deployment of the Seismometer to Investigate Ice and Ocean Structure (SIIOS) on Gulkana Glacier, Alaska. *Seismological Research Letters*, *91*(3), 1901–1914. Retrieved from https://pubs.geoscienceworld.org/ssa/srl/article/91/3/1901/583165/The-Deployment-of-the-Seismometer-to-Investigatehttps://pubs.geoscienceworld.org/ssa/srl/article/583165/The-Deployment-of-the-Seismometer-to-Investigate doi: 10.1785/0220190328

McDougall, T. J., & Barker, P. M. (2011). Getting started with TEOS-10 and the Gibbs Seawater (GSW) oceanographic toolbox. *SCOR/IAPSO WG*, *127*, 1–28.

McEwen, A. S. (1986). Tidal reorientation and the fracturing of Jupiter's moon Europa. *Nature*, *321*(6065), 49–51. Retrieved from https://doi.org/10.1038/321049a0 doi: 10.1038/321049a0

McNutt, S. R. (1996). Seismic monitoring and eruption forecasting of volcanoes: a review of the state-of-the-art and case histories. In *Monitoring and mitigation of volcano hazards* (pp. 99–146). Springer.

McNutt, S. R., & Roman, D. C. (2015, 1). Volcanic Seismicity. *The Encyclopedia of Volcanoes*, 1011–1034. Retrieved from https://www.sciencedirect.com/science/article/pii/B9780123859389000596https://www.sciencedirect.com/science/article/pii/B9780123859389000596?via%3Dihub doi: 10.1016/B978-0-12-385938-9.00059-6

Millero, F. J., Feistel, R., Wright, D. G., & McDougall, T. J. (2008). The composition of standard seawater and the definition of the reference-composition salinity scale. *Deep Sea Research Part I: Oceanographic Research Papers*, *55*(1), 50–72.

Mimoun, D., Murdoch, N., Lognonné, P., Hurst, K., Pike, W. T., Hurley, J., ... Banerdt, W. B. (2017). The Noise Model of the SEIS Seismometer of the InSight Mission to Mars. *Space Science Reviews*, *211*(1), 383–428. Retrieved from https://doi.org/10.1007/s11214-017-0409-x doi: 10.1007/s11214-017-0409-x

Nakamura, Y. (1977). Seismic energy transmission in an intensively scattering environment. *Journal of Geophysics Zeitschrift Geophysik*, *43*, 389–399.

Nakamura, Y. (2005, 1). Farside deep moonquakes and deep interior of the Moon. *Journal of Geophysical Research*, *110*(E1), E01001. Retrieved from http://doi.wiley.com/10.1029/2004JE002332 doi: 10.1029/2004JE002332

Nimmo, F., & Schenk, P. (2006). Normal faulting on Europa: implications for ice shell properties. *Journal of Structural Geology*, *28*(12), 2194–2203. doi: 10.1016/j.jsg.2005.08.009

Nissen-Meyer, T., van Driel, M., Stähler, S. C., Hosseini, K., Hempel, S., Auer, L., ... Fournier, A. (2014). AxiSEM: broadband 3-D seismic wavefields in axisymmetric media. *Solid Earth*, *5*(1), 425–445. Retrieved from http://www.solid-earth.net/5/425/2014/ doi: 10.5194/se-5-425-2014

Nunn, C., Garcia, R. F., Nakamura, Y., Marusiak, A. G., Kawamura, T., Sun, D., ... Zhu, P. (2020, 8). Lunar Seismology: A Data and Instrumentation Review. *Space Science Reviews*, *216*(5), 89. Retrieved from http://link.springer.com/10.1007/s11214-020-00709-3 doi: 10.1007/s11214-020-00709-3

Nunn, C., Pike, W. T., Standley, I. M., Calcutt, S. B., Kedar, S., & Panning, M. P. (2021, 2). Standing on Apollo's Shoulders: A Microseismometer for the Moon. *The Planetary Science Journal*, *2*(1), 36. Retrieved from http://dx.doi.org/10.3847/PSJ/abd63bhttps://iopscience.iop.org/article/10.3847/PSJ/abd63b doi: 10.3847/PSJ/abd63b

Oberst, J. (1987). Unusually high stress drops associated with shallow moonquakes. *Journal of Geophysical Research*. doi: 10.1029/JB092iB02p01397

Panning, M. P., Lekic, V., Manga, M., Cammarano, F., & Romanowicz, B. (2006, 12). Long-period seismology on Europa: 2. Predicted seismic response. *Journal of Geophysical Research: Planets*, *111*(E12), n/a-n/a. Retrieved from http://doi.wiley.com/10.1029/2006JE002712 doi: 10.1029/2006JE002712

Panning, M. P., Pike, W. T., Lognonné, P., Banerdt, W. B., Murdoch, N., Banfield, D., ... Warren, T. (2020, 4). On-deck seismology: Lessons from InSight for future planetary seismology. *Journal of Geophysical Research: Planets*, *125*(4), e2019JE006353. Retrieved from https://onlinelibrary.wiley.com/doi/abs/10.1029/2019JE006353http://doi.wiley.com/10.1029/2019JE006353 doi: 10.1029/2019JE006353

Panning, M. P., Stähler, S. C., Vance, S. D., Kedar, S., Tsai, V. C., Pike, W. T., ... Lorenz, R. D. (2018, 1). Expected seismicity and the seismic noise environment of Europa. *Journal of Geophysical Research: Planets*, *123*(1), 163–179. Retrieved from http://doi.wiley.com/10.1002/2017JE005332http://onlinelibrary.wiley.com/doi/10.1002/2017JE005332/abstracthttp://onlinelibrary.wiley.com/doi/10.1002/2017JE005332/pdf doi: 10.1002/2017JE005332

Pappalardo, R. T., Vance, S. D., Bagenal, F., Bills, B. G., Blaney, D. L., Blankenship, D. D., ... Soderlund, K. M. (2013). Science potential from a Europa lander. *Astrobiology*, *13*(8), 740–773. Retrieved from http://www.ncbi.nlm.nih.gov/pubmed/23924246 doi: 10.1089/ast.2013.1003

Peterson, J. (1993). *Observations and modeling of seismic background noise* (Tech. Rep.). Albuquerque, New Mexico: U.S. Department of the Interior Geological Survey. Retrieved from http://www.mttmllr.com/ADS/DATA/peterson_usgs_seismic_noise_ofr93-322.pdf doi: 10.3133/ofr93322Open-FileReport93-322

Phillips, C. B., & Pappalardo, R. T. (2014). Europa Clipper mission concept: exploring Jupiter's ocean moon. *Eos, Transactions American Geophysical Union*, *95*(20), 165–167.

Quick, L. C., & Marsh, B. D. (2015). Constraining the thickness of Europa's water–ice shell: Insights from tidal dissipation and conductive cooling. *Icarus*, *253*, 16–24. Retrieved from https://www.sciencedirect.com/science/article/pii/S0019103515000688 doi: https://doi.org/10.1016/j.icarus.2015.02.016

Reynolds, R. T., Squyres, S. W., Colburn, D. S., & McKay, C. P. (1983, 11). On the habitability of Europa. *Icarus*, *56*(2), 246–254. Retrieved from https://linkinghub.elsevier.com/retrieve/pii/0019103583900374 doi: 10.1016/0019-1035(83)90037-4

Schenk, P. M., & Mckinnon, W. B. (1989). Fault Offsets and Lateral Crustal Movement on Europa - Evidence for a Mobile Ice Shell. *Icarus*, *79*(1), 75–100. doi: Doi10.1016/0019-1035(89)90109-7

Stähler, S. C., Panning, M. P., Vance, S. D., Lorenz, R. D., van Driel, M., Nissen-Meyer, T., ... Kedar, S. (2017). Seismic Wave Propagation in Icy Ocean Worlds. *Journal of Geophysical Research: Planets*, *123*(1), 206–232. Retrieved from http://onlinelibrary.wiley.com/doi/10.1002/2017JE005338/abstracthttp://onlinelibrary.wiley.com/doi/10.1002/2017JE005338/pdfhttps://doi.org/10.1002/2017JE005338 doi: 10.1002/2017JE005338

Tolstoy, M., Waldhauser, F., Bohnenstiehl, D. R., Weekly, R. T., & Kim, W.-Y. (2008). Seismic identification of along-axis hydrothermal flow on the East Pacific Rise. *Nature*, *451*(7175), 181–184. Retrieved from 10.1038/nature06424 doi: 10.1038/nature06424

Vance, S. D., Hand, K. P., & Pappalardo, R. T. (2016, 5). Geophysical controls of chemical disequilibria in Europa. *Geophysical Research Letters*, *43*(10), 4871–4879. Retrieved from https://doi.org/10.1002/2016GL068547 doi: 10.1002/2016GL068547

Vance, S. D., Kedar, S., Panning, M. P., Stähler, S. C., Bills, B. G., Lorenz, R. D., ... Rhoden, A. R. (2018, 1). Vital Signs: Seismology of Icy Ocean Worlds. *Astrobiology*, *18*(1), 37–53. Retrieved from http://online.liebertpub.com/doi/abs/10.1089/ast.2016.1612http://www.liebertpub.com/doi/10.1089/ast.2016.1612 doi: 10.1089/ast.2016.1612

Vance, S. D., Panning, M. P., Stähler, S., Cammarano, F., Bills, B. G., Tobie, G., ... Banerdt, B. (2018, 11). Geophysical Investigations of Habitability in Ice-Covered Ocean Worlds. *Journal of Geophysical Research: Planets*, *123*(1), 180–205. Retrieved from http://doi.wiley.com/10.1002/2017JE005341https://doi.org/10.1002/2017JE005341 doi: 10.1002/2017JE005341

van Driel, M., Krischer, L., Stähler, S. C., Hosseini, K., & Nissen-Meyer, T. (2015, 6). Instaseis: instant global seismograms based on a broadband waveform database. *Solid Earth*, *6*(2), 701–717. Retrieved from http://www.solid-earth.net/6/701/2015/ doi: 10.5194/se-6-701-2015

Vilella, K., Choblet, G., Tsao, W. E., & Deschamps, F. (2020). Tidally Heated Convection and the Occurrence of Melting in Icy Satellites: Application

602 to Europa. *Journal of Geophysical Research: Planets*, *125*(3), 1–21. doi:
603 10.1029/2019JE006248
604 Waite, J. H., Glein, C. R., Perryman, R. S., Teolis, B. D., Magee, B. A., Miller, G.,
605 ... Bolton, S. J. (2017). Cassini finds molecular hydrogen in the Enceladus
606 plume: Evidence for hydrothermal processes. *Science*, *356*(6334), 155–159. doi:
607 10.1126/science.aai8703
608 Zahnle, K., Schenk, P., Levison, H., & Dones, L. (2003). Cratering rates in the outer
609 Solar System. *Icarus*, *163*(2), 263–289. doi: 10.1016/S0019-1035(03)00048-4